Anal. Chem. **2009,** *81,* 3035–3041

Detection of Extracellular H_2O_2 Released from Human Liver Cancer Cells Based on TiO_2 Nanoneedles with Enhanced Electron Transfer of Cytochrome *c*

Yongping Luo, Haiqing Liu, Qi Rui, and Yang Tian*

Department of Chemistry, Tongji University, Siping Road 1239, Shanghai 200092, P. R. China

The high conductive TiO_2 nanoneedles film is first employed as a support matrix for immobilizing model enzyme, cytochrome *c* (cyt *c*) to facilitate the electron transfer between redox enzymes and electrodes. Reversible and direct electron transfer of cyt *c* is successfully achieved at the nanostructured TiO_2 surface with the redox formal potential ($E^{0\prime}$) of 108.0 ± 1.9 mV versus Ag|AgCl and heterogeneous electron transfer rate constant (k_s) of 13.8 ± 2.1 s^{-1}. Experimental data indicate that cyt *c* is stably immobilized onto the TiO_2 nanoneedles film and maintains inherent enzymatic activity toward H_2O_2. On the basis of these results, the cyt *c*−TiO_2 nanocomposits film is capable of sensing H_2O_2 at a suitable potential, 0.0 V (vs Ag|AgCl), where not only common anodic interferences like ascorbic acid, uric acid, 3,4-dihydroxyphenylacetic acid but also a cathodic interference, O_2, are effectively avoided. Besides high selectivity, the present biosensor for H_2O_2 shows broad dynamic range and low detection limit. These remarkable analytical advantages, as well as the characteristic of TiO_2 nanoneedles film such as high conductivity, biocompatibility, and facile ability to miniaturize establishes a novel approach to detection of extracellular H_2O_2 released from human liver cancer cells.

Reactive oxygen species (ROS), including superoxide anion ($O_2^{\bullet-}$), hydrogen peroxide (H_2O_2), hydroxyl radical ($^{\bullet}OH$), peroxynitrite ($ONOO^-$), and so on has gained increasing attention in a variety of research fields, because they are considered as the mediators of the biochemistry of cellular pathology and may be involved in the etiology of aging and progressive neurodegenerative diseases, such as Parkinson's disease.[1−7] Under normal metabolic conditions, ROS is produced at a rate which is matched by the capacity of tissue to catabolize them. When its production exceeds the body's natural ability to deal with the potentially cytotoxic species, a variety of pathological conditions may result, including cancer, stroke, and neurodegeneration.[8,9]

Among the ROS, H_2O_2 is the most stable species and can diffuse across membranes through water channels and cause oxidative protein modifications at distal areas from its production.[10] H_2O_2 is one of the productions of $O_2^{\bullet-}$ dismutation from superoxide dismutase (SOD),[11] and forms $^{\bullet}OH$ in the presence of transition metals such as iron and copper (Fenton reaction).[12] As a consequence, the physiological levels of H_2O_2 are closely associated with the degradation and formation of reactive free radials, such as $O_2^{\bullet-}$ and $^{\bullet}OH$.[13] Therefore, a selective and sensitive method for reliable and durable determination of H_2O_2 with abroad linear range is essential and very useful for gaining a full understanding of the role that H_2O_2 and ROS play in pathology and physiology and the relationship between H_2O_2 and environmental stresses and lipid peroxidation.

Over the past years, considerable efforts have been paid on the development of electrochemical methods for determination of H_2O_2 due to their direct and real-time measurements.[14] Mostly, the third-generation biosensors for H_2O_2 based on direct electron transfer of proteins have paved an elegant way

* To whom correspondence should be addressed. E-mail: yangtian@mail.tongji.edu.cn. Phone: +86-21-65987075. Fax: +86-21-65982287.

(1) Halliwell, B. *J. Neurochem.* **1992**, *59*, 1609–1623.
(2) Hall, E.; Braughler, D. J. M. *Free Radical Biol. Med.* **1989**, *6*, 303–313.
(3) Maruyama, W.; Dostert, P.; Matsubara, K.; Naoi, M. *Free Radical Biol. Med.* **1995**, *19*, 67–75.
(4) Amatore, C.; Arbault, S.; Bruce, D.; Oliveira, P.; Erard, M.; Vuillaume, M. *Chem.—Eur. J.* **2001**, *7*, 4171–4179.
(5) Amatore, C.; Arbault, S.; Bouton, C.; Coffi, K.; Drapier, J.; Ghandour, H.; Tong, Y. *ChemBioChem* **2006**, *7*, 653–661.
(6) Amatore, C.; Arbault, S.; Bouton, C.; Drapier, J.; Ghandour, H.; Koh, A. C. K. *ChemBioChem* **2008**, *9*, 1472–1480.
(7) Shimanovich, R.; Groves, J. T. *Arch. Biochem. Biophys.* **2001**, *387*, 307–317.
(8) Van Lente, F. *Anal. Chem.* **1993**, *65*, 374R–377R.
(9) Halliwell, B.; Gutteridge, J. M. C. *Arch. Biochem. Biophys.* **1986**, *246*, 501–514.
(10) Henzler, T.; Steudle, E. *J. Exp. Bot.* **2000**, *51*, 2053–2059.
(11) McCord, J. M.; Fridovich, I. *J. Biol. Chem.* **1969**, *244*, 6049–6055.
(12) Theruvathu, J. A.; Aravindakumar, C.; Flyunt, T. R.; von Sonntag, J.; von Sonntag, C. *J. Am. Chem. Soc.* **2001**, *123*, 9007–9014.
(13) Mao, L.; Osbome, P. G.; Yamamoto, K.; Kato, T. *Anal. Chem.* **2002**, *74*, 3684–3689.
(14) (a) Gu, H.; Yu, A.; Chen, H. *J. Electroanal. Chem.* **2001**, *516*, 119–126. (b) Lei, C.; Hu, S.; Shen, G.; Yu, R. *Talanta* **2003**, *59*, 981–988. (c) Tatsuma, T.; Ogawa, T.; Sato, R.; Oyama, N. *J. Electroanal. Chem.* **2001**, *501*, 180–185. (d) Dong, S.; Li, J. *Bioelectrochem. Bioenerg.* **1997**, *42*, 7–13. (e) Miah, M.; Ohsaka, T. *Anal. Chem.* **2006**, *78*, 1200–1205. (f) Tatsuma, T.; Watanabe, T. *Anal. Chem.* **1991**, *63*, 1580–1585. (g) Tatsuma, T.; Watanabe, T.; Tatsuma, S.; Watanabe, T. *Anal. Chem.* **1994**, *66*, 290–294.
(15) (a) Zhang, L. *Biosens. Bioelectron.* **2008**, *23*, 1610–1615. (b) Xiang, C.; Zou, Y.; Sun, L.; Xu, F. *Electrochem. Commun.* **2008**, *10*, 38–41. (c) Jiang, X.; Zhang, L.; Dong, S. *Electrochem. Commun.* **2006**, *8*, 1137–1141. (d) Wang, J.; Li, M.; Shi, Z.; Li, N.; Gu, Z. *Anal. Chem.* **2002**, *74*, 1993–1997. (e) Zhou, Y.; Zhi, J.; Zou, Y.; Zhang, W.; Lee, S. *Anal. Chem.* **2008**, *80*, 4141–4146.

10.1021/ac802721x CCC: $40.75
Published on Web 03/16/2009

to detect H_2O_2 due to excellent selectivity and high sensitivity, in which cytochrome *c* (cyt *c*),[15] horseradish peroxidase (HRP),[16] myoglobin (Mb),[17] and hemoglobin (Hb)[18] were widely employed. For construction of enzyme-based third-generation biosensors for H_2O_2, an amount of effort have been made on the direct electron transfer of enzymes, since direct contact between enzymes and electrodes leads to significant structural and/or functional changes of the enzymes.[19] Cytochrome *c* is an excellent model for studying the electron transfer of typical enzymes from a structure point of view. In addition, in the view of further applications, a cyt *c*-based H_2O_2 biosensor is capable of avoiding the interference of O_2 under a reasonable applied potential, since cyt *c* is not a specific protein for O_2, unlike Hb and Mb which are the carriers of O_2 in biological systems. Therefore, in the past couple of decades, numerous applications of chemically or nonchemically modified methods to direct electron transfer of cyt *c* have been exploited.[20,21] With the development of nanostructured materials, Natan et al. did the pioneering work to realize reversible electrochemistry of cyt *c* with 12 nm diameter gold nanoparticles (AuNPs) and suggested that the size of AuNPs plays an important role in protein electrochemistry.[22] We have successfully fabricated three kinds of gold nanostructures and realized the direct and reversible electron transfer of cyt *c* at nanopyramidal and nanorodlike gold surfaces. Meanwhile, cyt *c* processes the biological activity after being immobilized on nanopyramidal and nanorodlike surfaces. Subsequently, the third-generation biosensor for H_2O_2 has been achieved with a linear detection range of 5 μM$\sim$1.5 mM at the applied potential of -100 mV versus Ag|AgCl.[23]

In view of the practical applications, the above H_2O_2 biosensor is still up against the following requirements: one is selectivity, another is linear detection range. An H_2O_2 sensor for use in a biological system must overcome great interferences from other species, in particular ascorbic acid (AA) and the changes in the endogenous levels of O_2 that are associated with the formation of H_2O_2 under pathophysiological conditions.[24] With most of the third-generation H_2O_2 biosensors which are based on direct electron transfer of proteins with high selectivity and sensitivity, including our above-mentioned H_2O_2 biosensor, it is easy to avoid the anodic interferences like AA, uric acid (UA), and 3,4-dihydroxyphenylacetic acid (DOPAC). However, the reductive potential of O_2 is commonly more positive than that of H_2O_2; therefore, it is very hard to detect H_2O_2 free from the interference of O_2 at those negative potentials, regardless that O_2 exists extensively in the biological system and is associated with the formation of H_2O_2. On the other hand, under normal physiological conditions, H_2O_2 holds a rather low physiological concentration. Increases in the activity of H_2O_2 occur in response to traumatic brain injury ischemia-reperfusion, environmental stresses, and so on, and the concentration of H_2O_2 may increase to $\sim10^{-3}$ M. Therefore, it is very essential to provide quantitative information on H_2O_2 concentration in a broad linear range for tracking the role that H_2O_2 plays in physiological and pathological processes.

In order to challenge these key analytical problems, in the present work, it is the first time that direct electron transfer of cyt *c* was exploited at a highly conductive TiO_2 nanoneedles surface with a formal potential of 108.0 ± 1.9 mV versus Ag|AgCl. A combination of direct electrochemistry of cyt *c* at TiO_2 nanoneedles and enzymatic catalytic activity of cyt *c* toward H_2O_2 paved a way for constructing a third-generation H_2O_2 biosensor. As a matter of fact, the analytical properties, in particular selectivity and sensitivity of electrochemical biosensors, are strongly dependent on the applied potentials of the biosensors. For the biosensors for H_2O_2 based on the direct electron transfer of proteins, the redox formal potentials of proteins play the key role in choosing the applied potentials of H_2O_2 biosensors. The more positive redox potential of cyt *c* obtained at the present TiO_2 nanoneedles, in particular the more positive reductive potential of oxidized cyt *c*, compared with those of proteins at SiO_2, TiO_2, and ZnO surfaces[25−27] is greatly benefits for the cathodic detection of H_2O_2 with a relatively high selectivity, avoiding not only anodic interferences like AA, UA, and DOPAC but also more importantly cathodic interference, O_2. Besides high selectivity, the present H_2O_2 biosensor exhibited other excellent analytical performances: broad dynamic linear range from 10^{-7} to 10^{-2} M, relatively long stability, and good reproducibility. These characteristics, together with the remarkable properties of the nanostructured TiO_2 film, sufficiently opened an electrochemical way to the determination of extracellular H_2O_2 from human liver cancer cells.

(16) (a) Mao, L.; Yamamoto, K. *Talanta* **2000**, *51*, 187–195. (b) Ferapontova, E.; Gorton, L. *Bioelectrochemistry* **2002**, *55*, 83–87. (c) Karyakin, A. A.; Karyakina, E. E.; Gorton, L. *Anal. Chem.* **2000**, *72*, 1720–1723. (d) Kenausis, G.; Chen, Q.; Heller, A. *Anal. Chem.* **1997**, *69*, 1054–1060.

(17) (a) Dai, Z.; Xu, X.; Ju, H. *Anal. Biochem.* **2004**, *332*, 23–28. (b) Zhang, H.; Hu, N. *J. Phys. Chem. B* **2007**, *111*, 10583–10590. (c) Liu, A.; Wei, M.; Honma, I.; Zhou, H. *Anal. Chem.* **2005**, *77*, 8068–8074. (d) Vaze, A.; Parizo, M.; Rusling, J. F. *Langmuir* **2004**, *20*, 10943–10948. (e) Li, N.; Xu, J.; Yao, H.; Zhu, J.; Chen, H. *J. Phys. Chem. B* **2006**, *110*, 11561–11565.

(18) (a) Liu, H.; Rusling, J. F.; Hu, N. *Langmuir* **2004**, *20*, 10700–10705. (b) Shi, G.; Sun, Z.; Liu, M.; Zhang, L.; Liu, Y.; Qu, Y.; Jin, L. *Anal. Chem.* **2007**, *79*, 3581–3588. (c) Sun, W.; Gao, R.; Jiao, K. *J. Phys. Chem. B* **2007**, *111*, 4560–4567. (d) Lu, X.; Hu, J.; Yao, X.; Li, J. *Biomacromolecules* **2006**, *7*, 975–980.

(19) (a) Holt, R. E.; Cotton, T. M. *J. Am. Chem. Soc.* **1989**, *111*, 2815–2821. (b) Yang, M. F.; Chung, L.; Thompson, M. *Anal. Chem.* **1993**, *65*, 3713–3716.

(20) (a) Eddows, M. J.; Hill, H. A. O. *J. Chem. Soc., Chem. Commun.* **1977**, *21*, 771–772. (b) Eddows, M. J.; Hill, H. A. O. *J. Am. Chem. Soc.* **1979**, *101*, 4461–4464. (c) Oliver, B. N.; Egekeze, J. O.; Murray, R. W. *J. Am. Chem. Soc.* **1988**, *110*, 2321–2322. (d) Taniguchi, I.; Iseki, M.; Toyosawa, K.; Yamaguchi, I.; Yasukouchi, K. *J. Electroanal. Chem.* **1984**, *164*, 385–391.

(21) (a) Jiang, X.; Shang, L.; Wang, Y.; Dong, S. *Biomacromolecules* **2005**, *6*, 3030–3036. (b) Yu, J.; Ju, H. *Anal. Chem.* **2002**, *74*, 3579–3583. (c) Wang, L.; Wang, E. *Electrochem. Commun.* **2004**, *6*, 49–54.

(22) Brown, K. R.; Fox, A. P.; Natan, M. J. *J. Am. Chem. Soc.* **1996**, *118*, 1154–1157.

(23) (a) Tian, Y.; Liu, H.; Zhao, G.; Tatsuma, T. *J. Phys. Chem. B* **2006**, *110*, 23478–23481. (b) Tian, Y.; Liu, H.; Deng, Z. *Chem. Mater.* **2006**, *18*, 5820–5822. (c) Liu, H.; Tian, Y.; Xia, P. *Langmuir* **2008**, *24*, 6359–6366. (d) Liu, H.; Tian, Y.; Deng, Z. *Langmuir* **2007**, *23*, 9487–9494.

(24) (a) Hyslop, P. A.; Zhang, Z.; Pearson, D. V.; Phebus, P. L. *Brain. Res.* **1995**, *671*, 181–186. (b) Marzouk, S. A. M.; Ufer, S.; Buck, R. P.; Johnson, T. A.; Dunlap, L. A.; Cascio, W. E. *Anal. Chem.* **1998**, *70*, 5054–5061.

(25) (a) Yao, H.; Li, N.; Xu, S.; Xu, J.; Zhu, J.; Chen, H. *Biosens. Bioelectron.* **2005**, *21*, 372–377. (b) Zhang, H.; Zou, X.; Han, D. *Anal. Lett.* **2007**, *40*, 661–676.

(26) (a) Zheng, W.; Zheng, Y.; Jin, K.; Wang, N. *Talanta* **2008**, *74*, 1414–1419. (b) Liu, A.; Wei, M.; Honma, I.; Zhou, H. *Anal. Chem.* **2005**, *77*, 8068–8077. (c) Zhang, L.; Zhang, Q.; Li, J. *Adv. Funct. Mater.* **2007**, *17*, 1958–1965. (d) Zhang, Y.; He, P.; Hu, N. *Electrochim. Acta* **2004**, *49*, 1981–1988. (e) Xiao, P.; Garcia, B. B.; Guo, Q.; Liu, D.; Cao, G. *Electrochem. Commun.* **2007**, *9*, 2441–2447. (f) Lu, H.; Yang, J.; Rusling, J. F.; Hu, N. *Electroanalysis* **2006**, *18*, 379–390.

(27) (a) Lin, K.; Chen, S. *Biosens. Bioelectron.* **2006**, *21*, 1737–1745. (b) Zhao, G.; Xu, J.; Chen, H. *Anal. Biochem.* **2006**, *350*, 145–150.

EXPERIMENTAL SECTION

Chemicals and Materials. UA was purchased from Alfa Aesar, and AA, DOPAC, KNO_3, $NaNO_2$, and Na_2SO_3 were obtained from Sinopharm Chemical Reagent Co., Ltd. Horse heart cyt *c* (MW 13 000) was obtained from Sigma and used as received. Other reagents were of analytical grade and used as received. All the solutions were prepared with Milli-Q water and were deaerated with high purity nitrogen before experiments. Indium tin oxide (ITO)-coated glass plates with a square resistance of ~10 Ω cm^{-2} were obtained from Shenzhen Nanbo Display Technology Co. Ltd. (Shenzhen, China). All electrochemical experiments were carried out at room temperature.

Preparation and Modification of TiO_2 Nanoneedles Film. ITO-coated glass plates were thoroughly cleaned in the following solvents: soapy water, neat ethanol, 1 M NaOH, and water. A nanoneedles film was prepared by coated nanoneedles TiO_2 sol onto an ITO glass plates by the spin-coating method and then sintered at 723 K for 1 h. The nanostructured TiO_2 film was modified with cyt *c* by immersing the TiO_2 film into a phosphate buffered-saline (PBS) solution (pH 7.0) of cyt *c* (0.2 mM) for about 0.5−3 h at 3 °C in the refrigerator. Hereafter, the cyt *c* modified-nanostructured TiO_2 electrode will be referred as TiO_2/cyt *c*.

Apparatus and Measurements. SEM images were taken by a Quanta 200 FEG (FEI Company). The UV−vis absorption spectrum was recorded by an Agilent 8453 UV−vis-NIR spectrophotometer (Agilent Instruments). CHI 660 and CHI 832 electrochemical work stations (CH Instruments) were employed in all electrochemical measurements, which were carried out with a three-electrode electrochemical cell. The reference electrode was a KCl-saturated Ag|AgCl electrode, while the auxiliary electrode was a platinum wire.

Detection of Extracellular H_2O_2. Human liver cancer cell lines Hep G2 were obtained from Japanese Cancer Research Resources Bank (Tokyo, Japan). The cells were maintained in a culture medium consisting of Delbecco's modified minimum essential medium (DMEM; Wako Pure Chemicals, Japan) and subcultured every 5 days. The Hep G2 cells were centrifuged to obtain a cell-packed pellet ($1.0-1.5 \times 10^5$ cells cm^{-2}) for the electrochemical experiments. Real sample measurements were performed in PBS containing 100 mM glucose. The device was viewed under a microscope.

RESULTS AND DISCUSSION

Surface Properties of the TiO_2 Nanoneedles Film. The morphology of a TiO_2 nanoneedles film was characterized by scanning electron microscopy (SEM). As demonstrated in Figure 1, the TiO_2 nanoneedles are typically ~50−100 nm in width and ~3−5 μm in length and almost homogenously disperse on a whole sheet.

To characterize the electrochemical properties of the nanostructured TiO_2 surface, cyclic voltammetry of an electron transfer indicator like $Fe(CN)_6^{3-/4-}$ was studied at the TiO_2 nanoneedles electrode, compared to that at an ITO substrate. The surface of TiO_2 was considered to be covered with hydroxyl groups. Therefore, the TiO_2 surface covered with hydroxyl groups exhibits a negative charge at pH 7.0, which is supported by comparison with the electrochemical response of $Fe(CN)_6^{3-/4-}$ at the TiO_2 nanoneedles film and

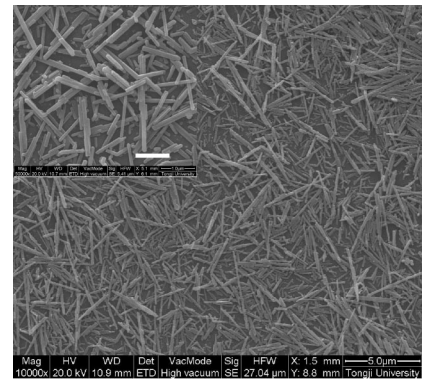

Figure 1. SEM images of TiO_2 nanoneedles film. The bar demonstrated in the inset corresponds to 1.0 μm.

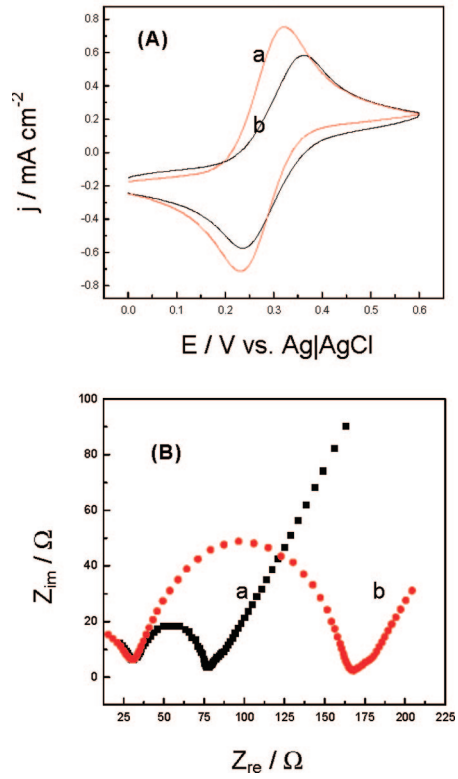

Figure 2. (A) Cyclic voltammograms (CVs) obtained at ITO (a) and the nanostructured TiO_2 surface (b) in 0.1 M KCl solution containing 1 mM $[Fe(CN)_6]^{3-/4-}$. Potential scan rate: 100 mV s^{-1}. (B) Nyquist plots of $[Fe(CN)_6]^{3-/4-}$ obtained at ITO (a) and the nanostructured TiO_2 surface (b).

bare ITO electrode, as depicted in Figure 2A. A severe decrease in the redox peak and a great widening of the peak-to-peak separation (ΔE_p) was observed at the TiO_2 nanoneedles film, which may be ascribed to the electrostatic repulsion between the $Fe(CN)_6^{3-}$ or $Fe(CN)_6^{4-}$ anion and the negatively charged nanostructured TiO_2 surface. This result was further confirmed by electrochemical impedance spectroscopy (EIS). The charge transfer resistance (R_{ct}) of the $Fe(CN)_6^{3-/4-}$ redox couple is near 50 Ω at the ITO substrate (Figure 2B, voltammogram a) but it increases to ~150 Ω at the nanostructured TiO_2 surface (Figure 2B, voltammogram b). The increase in the charge transfer resistance at the TiO_2 film, not only the resistance of film (R_{film}), suggests again that the negatively charged TiO_2 nanoneedles

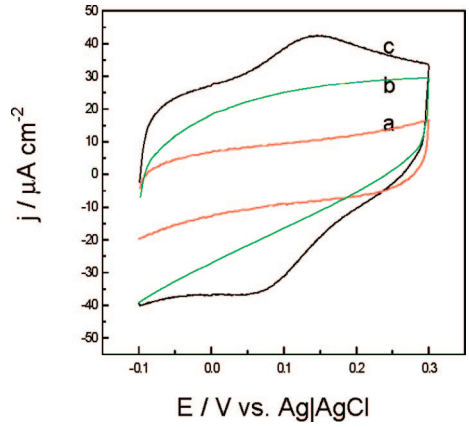

Figure 3. CVs obtained at the ITO substrate (a), bare TiO_2 nanoneedles film (b), and TiO_2/cyt *c* film (c) in 10 mM PBS (pH 7.0). Potential scan rate: 100 mV s^{-1}.

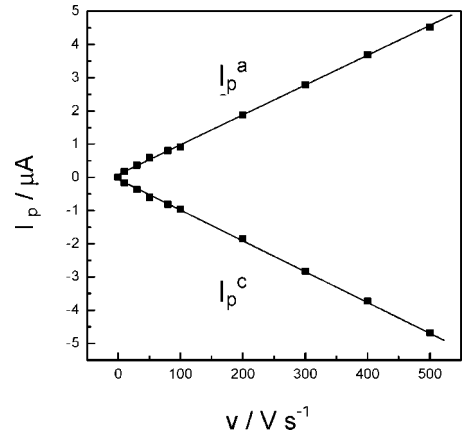

Figure 4. Relationship between anodic and cathodic peak currents of the TiO_2/cyt *c* film and potential scan rate.

surface inhibits the electron transfer of $Fe(CN)_6^{3-}$ and/or $Fe(CN)_6^{4-}$ anion due to electrostatic repulsion. On the other hand, at pH 7.0, cyt *c* with p*I* = 9.5 has a net positive charge. Therefore, the nanostructured TiO_2 surface with a negative charge may greatly benefit from the adsorption of cyt *c* molecules and subsequently enhance the electron transfer of cyt *c*.

Electrochemical and Spectroscopic Characterization of Cytochrome *c* at the TiO_2 Nanoneedles Film. As expected, a pair of well-defined redox peaks was observed at the TiO_2/cyt *c* surface (CV c), while only the charge current was obtained at either the ITO substrate (a) or the TiO_2 nanoneedles surface (b) in 10 mM PBS (pH 7.0) in the absence of cyt *c* (Figure 3). The formal potential ($E^{0\prime} = (E_{p,a} + E_{p,c})/2$) of cyt *c* obtained at the TiO_2 nanoneedles film is estimated to be 108.0 ± 1.9 mV ($n = 4$) versus Ag|AgCl and a peak width at half-peak height ($\Delta E_{p,1/2}$) of ΔE_p is calculated to be 68.3 ± 2.7 mV ($n = 4$).

CVs of the TiO_2/cyt *c* electrode at various scan rates were also obtained in fresh buffer solution in the absence of cyt *c* (Supporting Information, Figure S1). As demonstrated in Figure 4, both the anodic and cathodic peak currents (I_p^a and I_p^c) vary linearly with potential scan rate (v) suggest the

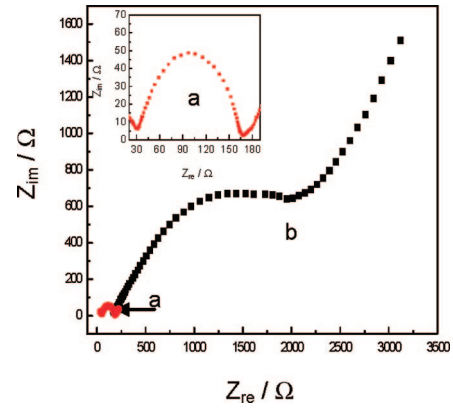

Figure 5. Nyquist plots obtained at the (a) bare TiO_2 nanoneedles film (enlarged in the inset) and (b) TiO_2/cyt *c* electrode in 0.1 M KCl solution containing 1 mM $[Fe(CN)_6]^{3-/4-}$.

surface-confined process. According to Laviron's equation,[28] the relevant kinetic parameters of the electrode reaction, i.e., the rate constant of the electrochemical process (k_s) and cathodic transfer coefficients (α_c), were calculated: $k_s = 13.8 \pm 2.1$ s^{-1}, $\alpha_c = 0.47 \pm 0.02$ ($n = 4$) at the nanostructured TiO_2 surface. k_s of cyt *c* obtained at this nanostructured TiO_2 film is 1 order of magnitude greater than those obtained at TiO_2 nanotubes and other metal oxides surfaces, such as SnO_2, WO_3, ITO, and SiO_2 surfaces,[29] indicating that direct electron transfer of cyt *c* is remarkably enhanced at the TiO_2 nanoneedles surface. TiO_2/cyt *c* nanocomposites show reversible electrochemistry with formal potential of 108.0 ± 1.9 mV vs Ag|AgCl and a k_s value of 13.8 ± 2.1 s^{-1}.

Figure 5 shows the Nyquist plots obtained at the bare TiO_2 nanoneedles film and TiO_2/cyt *c* electrode in 0.1 M KCl solution containing 0.1 M $[Fe(CN)_6]^{3-/4-}$ to confirm the adsorbed behavior of cyt *c*. The charge transfer resistance (R_{ct}) of $Fe(CN)_6^{3-/4-}$ redox couple is about 137 Ω at TiO_2 nanoneedles film (a), but it increases to 1.9 KΩ after cyt *c* was immobilized on the nanostructured TiO_2 surface as (Figure 5b). These data suggested that cyt *c* adsorbed onto the nanostructured TiO_2 surface might inhibit the electrochemical communication between the electron transfer indicator, $Fe(CN)_6^{3-/4-}$and the TiO_2 nanoneedles electrode, resulting in a greater increase of the R_{ct} of the $Fe(CN)_6^{3-/4-}$ redox couple.

Next, it is desirable to clarify whether cyt *c* retains inherent activity toward H_2O_2 after immobilized on the TiO_2 nanostructures. The Soret band of heme protein is usually employed as an indicator of the microenvironment where the heme center is located. The peak will be diminished if the protein is denaturated.[30] Figure 6 depicts the UV−vis absorption spectra of 0.2 mM cyt *c* in solution (a) and cyt *c*

(28) Laviron, E. *J. Electroanal. Chem.* **1979**, *101*, 19–28.
(29) (a) Topoglidis, E.; Astuti, Y.; Duriaux, F.; Grtzel, M.; Durrant, J. R. *Langmuir* **2003**, *19*, 6894–6900. (b) Geng, R.; Zhao, G.; Liu, M.; Li, M. *Biomaterials* **2008**, *29*, 2794–2801. (c) Zhang, X.; Wang, J.; Wu, W.; Qian, S.; Man, Y. *Electrochem. Commun.* **2007**, *9*, 2098–2104. (d) Zhao, G.; Lei, Y.; Zhang, Y.; Li, H.; Liu, M. *J. Phys. Chem. C* **2008**, *112*, 14786–14795. (e) Lyon, J.; Hill, R.; Shear, J.; Stevenson, K. *Anal. Chem.* **2007**, *79*, 2303–2311. (f) Deng, Z.; Gong, Y.; Luo, Y.; Tian, Y. *Biosens. Bioelectron.* In press.
(30) (a) Nassar, A. F.; Willis, W. S.; Rusling, J. F. *Anal. Chem.* **1995**, *67*, 2386–2392. (b) Wang, C.; Yang, C.; Song, Y.; Gao, W.; Xia, X. *Adv. Funct. Mater.* **2005**, *15*, 1269–1275.

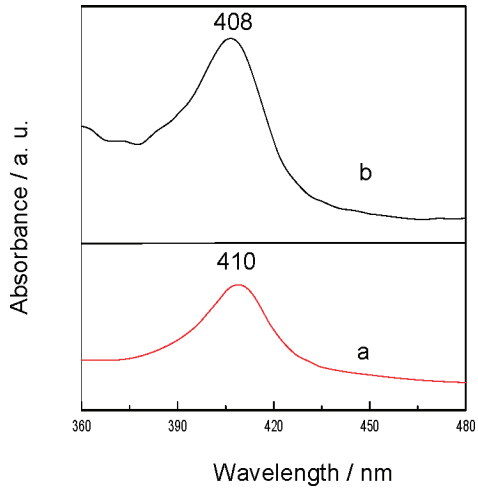

Figure 6. UV−vis absorption spectra of (a) 0.2 mM cyt *c* solution and (b) cyt *c* confined on the TiO_2 nanoneedles film.

confined on the optical transparent TiO_2 nanoneedles surface (b). The band for cyt *c* adsorbed on the nanostructured TiO_2 film is located at 408 nm, a 2 nm blue shift compared with that of the native cyt *c* solution (410 nm), revealing that cyt *c* almost processed its intrinsic activity toward H_2O_2 after adsorbed on the TiO_2 nanoneedles film.

Sensitivity and Selectivity of the H_2O_2 Biosensor. As demonstrated above, the direct electron transfer of cyt *c* was enhanced at the TiO_2 nanoneedles surface, and cyt *c* immobilized on the nanostructured TiO_2 film almost processed the enzymatic activity. These results provided a platform for constructing the third-generation biosensor for H_2O_2 because the heme has been well documented as the active site for the catalysis of the reduction of H_2O_2.

As a matter of fact, the sensitivity of electrochemical biosensors is strongly dependent on the applied potential. The present H_2O_2 biosensor is not an exception. The cathodic current intensity of H_2O_2 obtained at the TiO_2/cyt *c* film increased with the negative shift of the operating potentials (Supporting Information, Figure S2). This observation indicates that the more negative the operating potential, the higher sensitivity the H_2O_2 biosensor shows. On the other hand, selectivity of electrochemical biosensors is also potential-dependent. Figure 7 demonstrates seven kinds of potential interferences under different applied potentials. Similar to the H_2O_2 biosensors previously reported, at the negative potentials, e.g., −0.05 and −0.1 V, the present H_2O_2 biosensor were free from the anodic interferences like AA, UA, DOPAC, NO_2^-, NO_3^-, and SO_3^{2-}, but 0.84 and 1.91% of cathodic response currents of 200 μM O_2 were observed relative to 100 μM H_2O_2. On the other hand, at the positive potentials +0.05 and +0.1 V, 10.88 and 18.95% of anodic currents of 100 μM AA were obtained relative to 100 μM H_2O_2. Fortunately, at the suitable potential of 0.0 V, both anodic and cathodic potential interferences were negligible. Therefore, for fulfillment of both the selectivity and sensitivity of the present biosensor, 0.0 V (vs Ag|AgCl) was selected as the optimized operating potential.

Linear Range, Detection Limit, and Stability. Amperometric responses of TiO_2 nanoneedles and TiO_2/cyt *c* films to

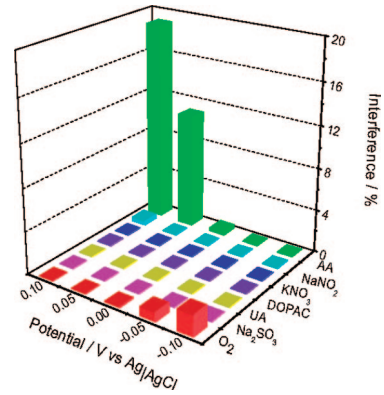

Figure 7. The selectivity profile of the present H_2O_2 biosensor obtained at different applied potentials: −0.10, −0.05, 0.00, 0.05, 0.10 V versus Ag/AgCl.

successive concentration changes of H_2O_2 were conducted at the optimized potential of 0.0 V, and the corresponding current−time responses are shown in Figure 8A. No response was observed at the bare TiO_2 nanoneedles surface, while well-defined steady-state current responses were obtained and the currents increased stepwise with successive additions of H_2O_2. The calibration plot of steady-state currents obtained at the TiO_2/cyt *c* film against concentration of H_2O_2 is depicted in Figure 8B. The analytical performance of the present H_2O_2 biosensor at the optimum conditions was summarized in Table 1. For comparison, other previously attained third-generation H_2O_2 biosensors based on direct electron transfer of proteins at nanostructured TiO_2 or titanate nanostructures[26] were also listed in Table 1. Compared with other H_2O_2 biosensors reported so far, besides higher selectivity, the present H_2O_2 biosensor shows excellent analytical performance, for instance, wider linear detection range and lower detection limit. In particular, the dynamic linear range for detection of H_2O_2 from 8.5×10^{-7} to 2.4×10^{-2} M at the applied potential of 0.0 V, is greatly wider than those obtained in previous H_2O_2 biosensors and fulfill the requirement of in vivo or online tracking of H_2O_2 concentration.

The TiO_2/cty *c* electrode was stored in a black box at 3 °C in the refrigerator between tests for avoiding light irradiation. The response current for H_2O_2 was recorded three times daily, and the current responses had almost no changes for at least 1 month, indicating the good stability of the present biosensor. Moreover, the deviation of the current responses of over 10 sensors prepared with the same method did not exceed 5.8% (RSD).

Detection of Extracellular H_2O_2 Released from Human Liver Cancer Cells. Figure 9 depicts amperometric responses obtained at the (a) TiO_2 nanoneedles film and (b) TiO_2/cty *c* electrode located near the human liver cancer cell lines Hep G2 in 10 mM PBS (pH 7.0) containing 100 mM glucose at the applied potential of 0.0 V vs Ag|AgCl after the injection of (A) 10 mM phobol 12-myristate-13-acetate (PMA) and (B) 300 U mL^{-1} catalase. The increased cathodic current was observed at the TiO_2/cyt *c* electrode with the addition of PMA, which was reported to induce H_2O_2 production from

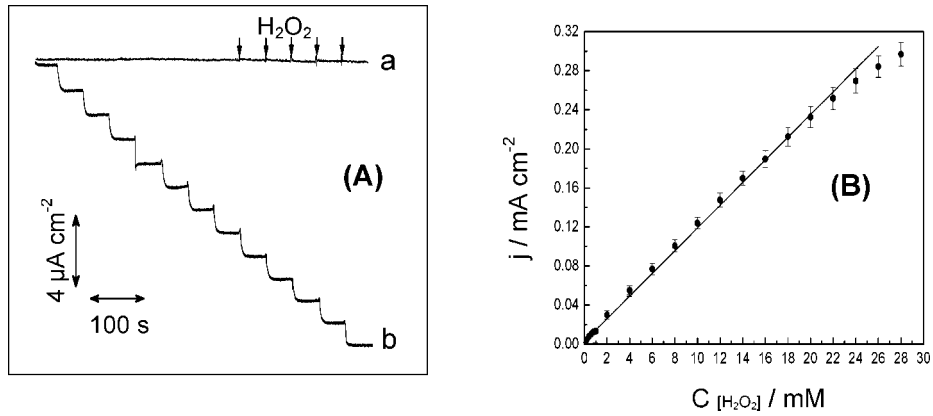

Figure 8. (A) Typical amperometric responses of (a) the TiO_2 nanoneedles film and (b) the TiO_2/cyt *c* film to successive additions of 100 μM H_2O_2 at applied potentials of 0.0 V versus Ag|AgCl in 10 mM PBS (pH 7.0). (B) Calibration plot of steady-state currents obtained at the TiO_2/cyt *c* electrode against concentrations of H_2O_2.

Table 1. Analytical Performance of the H_2O_2 Biosensor Based on TiO_2/Cytochrome *c* Nanocomposites

nanocomposites	potential (mV vs SCE)	linear range (μM)	detection limit (μM)	ref
cytochrome *c*/TiO_2 nanoneedles	−45 (0.0 V vs Ag|AgCl)	0.85−24 000	0.26	[a]
Hb/CMC-TiO_2 nanotubes	−300	4−64	4.637	26a
Mb/titanate nanotubes	(CV peak potential) ∼−290	2−160	0.6	26b
Mb/titanate nanosheets	(CV peak potential) ∼−310	2−160	0.6	26c
HRP/TiO_2 nanoparticles	0	7.5−123	2.5	26d
HRP/Th-TiO_2 nanotubes	−645	10−3000		26e
HRP-PMS-TiO_2 sol−gel	−250	4−1000	0.8	26f

[a] The present work.

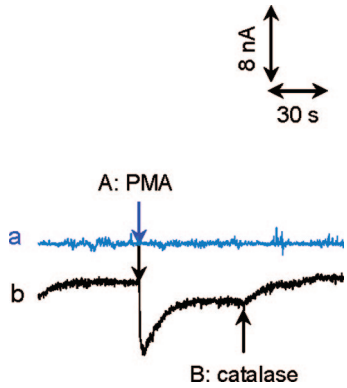

Figure 9. Amperometric responses obtained at the (a) TiO_2 nanoneedles film and (b) TiO_2/cyt *c* electrode in 10 mM PBS (pH 7.0) containing 100 mM glucose at the applied potential of 0.0 V vs Ag|AgCl with the addition of (A) 10 mM PMA and (B) 300 U mL^{-1} catalase.

the cells,[31] and a reduction current of ∼4.9 nA was obtained in 20 s, while no response was attained at bare TiO_2 nanoneedles film with the same addition of PMA. In addition, after injected 300 U mL^{-1} catalase solution, a selective scavenger of H_2O_2 into the solution, the current shown in curve b decreased down to almost the background. Accordingly, we can conclude that the generated increase of cathodic current at the TiO_2/cyt *c* electrode located near the cells is ascribed to the enzymatic reduction of H_2O_2, which is effectively mediated by the cyt *c* confined on the electrode. This observation substantially demonstrates that the presently developed third-generation H_2O_2 biosensor with a nanostructured TiO_2 surface establishes an approach for reliable and durable determination of extracellular H_2O_2 and could be potentially useful for further physiological and pathological investigations.

CONCLUSIONS

Direct and fast electron transfer of cyt *c*, an excellent model for investigation of the electron transfer of enzymes, was first exploited at the highly conductive TiO_2 nanoneedles surface. The formal potential was estimated to be 108.0 ± 1.9 mV (vs Ag|AgCl), and the electrochemical process was reversible with a heterogeneous electron transfer rate constant of 13.8 ± 2.1 s^{-1}. Experimental results revealed that cyt *c* was stably confined onto the nanostructured TiO_2 film, and spectroscopic data suggested that cyt *c* held inherent enzymatic activity toward H_2O_2. On the basis of these experimental results, an H_2O_2 biosensor was developed with high selectivity, free from not only anodic interferences, including UA, AA, and DOPAC, but also cathodic interference, O_2. Besides this advantage, the present H_2O_2 biosensor exhibited a broad dynamic linear range and low detection limit. The striking analytical characteristics, together with the intrinsic properties of TiO_2 nanostructures, such as biocompatibility, easy to prepare, and facile miniaturization, sufficiently offered an electrochemical approach to determine extracellular H_2O_2 released from human liver cancer cells. This investigation not only provided a methodology for the direct electron

(31) Lin, Q.; Jin, L.; Cao, Z.; Lu, Y.; Xue, H.; Xu, Y. *Phytother. Res.* **2008**, *22*, 740–745.

transfer of enzymes on the nanostructured semiconductors, and on the basis of this platform to construct biosensors for ROS, but also established a novel approach for durable and reliable detection of H_2O_2 in the biological system.

ACKNOWLEDGMENT

We are grateful to Dr. K. Komori at the University of Tokyo for the cell preparations and helpful discussion. This work was financially supported by the Program for New Century Excellent Talents in University (Grant NCET-06-0380) and the Scientific Research Foundation for the Returned Overseas Chinese Scholars from State Education Ministry, China.

SUPPORTING INFORMATION AVAILABLE

Additional information as noted in text. This material is available free of charge via the Internet at http://pubs.acs.org.

Received for review December 22, 2008. Accepted February 21, 2009.

AC802721X